Spirometer Techniques for Measuring Molar Composition in Argon Carbon Dioxide Mixtures

by

Daniel Burje Chonde

Submitted to the Department of Physics
in partial fulfillment of the requirements for the degree of

Bachelor of Science in Physics

at the

MASSACHUSETTS INSTITUTE OF TECHNOLOGY

May 2007
[June 2007]

Author .....
Department of Physics
May 18, 2007

Certified by .....
Peter Fisher
Division Head, Particle and Nuclear Experimental Physics
Thesis Supervisor

Accepted by .....
David E. Pritchard
Senior Thesis Coordinator, Department of Physics

Spirometer Techniques for Measuring Molar Composition in Argon Carbon Dioxide Mixtures

by

Daniel Burje Chonde

Submitted to the Department of Physics
on May 18, 2007, in partial fulfillment of the
requirements for the degree of
Bachelor of Science in Physics

Abstract

This paper examines a new technique for measuring gas composition through the use of a spirometer. A spirometer is high precision pressure transducer which measures the speed of sound in a gas through the emission and reception of ultrasonic pulses, commonly used in medicine to measure patient lung capacity. The spirometer was successfully calibrated to measure gas composition to an accuracy of $1.75\% \pm 1.23\%$ by ratio by weight. By using a spirometer, the speed of sound was measured for a trapped volume of Argon CO_2 mixtures at ratios of $80:20$, $85:15$, $90:10$, $95:5$, and $100:0$. The temperature dependence of the transit time was observed to behave according to the Laplace Formula, except for the presence of dramatic drops that were dependent on the Argon concentration. An argument is presented that these drops are technical limitations of the spirometer.

Thesis Supervisor: Peter Fisher
Title: Division Head, Particle and Nuclear Experimental Physics

Acknowledgments

I would like to acknowledge all of my professors at MIT for teaching me how to think, question, and understand our world; however, I would especially like to acknowledge Peter Fisher, for giving a freshman a chance, teaching me everything I know about lab, and letting me hang around until it was time for me to graduate.

While working at Building 44 these four years I have learned and accomplished more than I thought possible. I would like to thank Ben Monreal for his guidance, especially on this project; Prof. Ulrich Becker for his wisdom; Martina Green for her invaluable advice and help; Andrew Werner for teaching me the ropes; Sa Xiao for her invaluable ROOT script and her work on the theory; Kim Boddy for teaching me how to use ROOT; Gray Rybka for helping me fix everything I broke; Tim Hill for his technical expertise; as well as the rest of the 44 students, Gianpaolo Carosi, Tom Walker, Feng Zhou, it has been a pleasure working with all of you. I am especially indebted to Christine Titus and Mike Grossman for all of their help.

Finally, all of this would not have been possible without the support of my family, especially Mom, Dad, and my loving girlfriend Sun Yoo, for editing this and for being yourselves.

Contents

List of Figures

List of Tables

Chapter 1

Introduction

1.1 Alpha Magnetic Spectrometer

The Alpha Magnetic Spectrometer 02 (AMS02) is an experiment to search for dark matter, missing matter, and antimatter on the International Space Station (ISS). AMS02 measures the properties of cosmic rays in order to determine their composition. By measuring the properties of Cosmic rays, which are comprised of high energy particles and electromagnetic radiation, the cylindrical detector determines what particles the cosmic rays were comprised of. It is believed that dark matter and antimatter could be present in cosmic rays; therefore, any particle detected by AMS02 that has properties unlike any recorded particle must be one of those three types of matter. To say with certainty that a particle is unlike any known particle, AMS02 must make high precision measurements. AMS02 is comprised of nine separate detectors, each of which measures a separate property of the cosmic ray: the Transition Radiation Detector (TRD), two separate Time of Flight detectors, a Magnet, a Silicon tracker, an Anticoincidence counter, an Amiga Star tracker, a Ring Image Cherenkov Counter, and an Electromagnetic Calorimeter.

The first detector in AMS02 that the cosmic ray passes through is the Transition Radiation Detector (TRD). The TRD is designed to separate electron and proton signals to distinguish between positron and proton signals (as well as antiproton and electron signals). The TRD has a rejection factor of $10^3 - 10^2$ in the energy range of

$10 - 300$ GeV [1]. The detector is comprised of 20 layers of straw monitor tubes of 6 mm diameter. The wall material of the straw tubes is a 72 μm thick kapton-aluminum foil. The upper and lower four layers run parallel to the AMS magnetic field while the central wires run perpendicular, allowing the TRD to track the particle's trajectory. Alternating between the tubes are layers of polyethylene/polypropyleen fiber radiator. As a particle passes through the fiber radiator it produces transition radiation which is picked up by the straw tubes. The particle type is then determined by the signal. The transition radiation photon detection (i.e. the gain of the signal) is optimized by filling the tubes with a precise 80% to 20% mixture of Xe to CO_2 gas at 1 bar. Since Xe and CO_2 have different diffusion rates through the straw tubes, and the gas will be slowly leaking into space, the straw tubes need to be regularly replenished by an onboard supply. The gas mixture is produced onboard from a recirculating gas system. For the three year mission, AMS02 is equipped with 50kg of Xe and 5kg of CO_2 with a maximum of 7 L of gas being transferred to the buffer daily. For safety reasons, much of the gas supply system is automated. The gas system is comprised of a module for supply, a module for mixing, and manifolds to distribute the gas. Using high pressure valves and pressure sensors the gases are mixed using the law of partial pressures, similar to how commercial gas mixtures are made. For AMS02 to properly distinguish the particles the gas supply in the TRD must remain stable to within 3% [1]. To ensure that the deviations in the resulting mixture is within 3%, the composition of the gas that is passed to the manifolds must be checked. Since there are no current devices or precedent for measuring the gas composition for flowing gases, the molar composition of the gas is checked in a novel manner using a spirometer. This thesis suggests the feasibility for using a spirometer to measure gas composition.

1.2 Gas Production Process

Currently there is one method to mix gases with any type of precision, and once mixed there is no reliable method to check the mixtures composition. Using the idea that

partial pressures are proportional to molar ratios, gases are mixed using high precision pressure gauges. This is how the gases are mixed on AMS02, though on AMS02 the gases are initially pure and do not need to be separated from impure components. The pure gases are gathered in a number of ways. Gases like Argon are produced through cryogenic air separation since they are very prevalent in air. First the dry air is filtered and compressed to 90 psig. The air is then cooled to room temperature by passing through water-cooled and air-cooled heat exchanges or by passing through mechanical refrigeration systems. As it cools, condensed water is removed. After the gas is cooled the remaining water vapor and carbon dioxide are removed using molecular sieve units. These sieves are small process units that absorb carbon dioxide and water onto their surfaces. From there, the gas is placed in brazed aluminum heat exchangers that supercools the gas to approximately -185 Celsius. Once cooled, the gas is placed in distillation columns to separate the air into desired products. The lighter Nitrogen settles to the top while the heavier oxygen and argon settle to the bottom. The argon-oxygen mixture is then placed in another column where crude argon is vented into a catalyst-containing vessel where it is combined with hydrogen and then run through another sieve to remove the resulting water. Since the CO_2 concentrations are low in the atmosphere, CO_2 is produced from various byproduct streams of industrial processes. Each gas is then fed into a large chamber while measuring the pressure. Since the gas is mixed in large volumes, any small errors in pressure (and thus concentration) are shared over the whole volume, and can thus be neglected, so the mixture can be considered homogeneous. Even for a mixture of the highest purity Ar CO_2 gas mixtures, these errors in mixing can lead to a tolerance of 5% of the desired ratio. Though this production process can accurately produce mixtures of gases, it cannot be used to determine the mixture as gas is being flowed, which is a limitation of this process. In gaseous detectors, the uncertainty of the mixture is then a factor in the error. Using a spirometer, a high precision pressure transducer which measures the speed of sound in a gas through the emission and reception of ultrasonic pulses, the actual composition flowing from the gas cylinder to the apparatus can be accurately determined.

This thesis will examine the theory and a procedure for calibrating a spirometer to be used to determine the composition of a gas. Chapter 2 will focus on the theory of sound speed in different molecular gases and the sound speed's dependence on molar concentration. Chapters 3 and 4 will discuss and analyze a terrestrial experiment which will determine the feasibility for a spirometer to be used to determine gas composition on AMS02. Finally, the limitations of the spirometer will be discussed and conclusions will be drawn.

Chapter 2

Theory

Sound is the phenomenon of the propagation of longitudinal pressure disturbance waves through a medium. The distance traveled per unit time of the transverse wave packet is defined as the speed of sound, assuming that the disturbance does not deform over the distance. Resolving the disturbance into spatially harmonic components, at a given point the disturbance can be characterized by a phase angle, with which the distance traveled per unit time is referred to as the group velocity, whose magnitude is the speed of sound. It is the group velocity which determines the propagation of sound in a medium through the wave equation. If the group velocity is the same for all frequencies of disturbance, the medium is a nondispersive medium; otherwise it is a dispersive medium [2]. If the medium's size is much larger than the wave packet, in regions far from boundary conditions the speed of sound only depends on the properties of the medium and the harmonic frequencies of the propagating wave. Under these conditions, referred to as perfectly anechoic conditions, the wave exhibits free field propagation [2].

2.1 Laplace formula and its assumptions

Laplace derived a simple formula relating the speed of sound with the properties of a gaseous medium:

$$W_s^2 = \frac{\gamma_s RT}{M} \tag{2.1}$$

where W_s is the speed of sound, γ_s is the ratio of the specific heat at constant pressure to the specific heat at constant volume, C_p/C_v, R is the universal gas constant given by Avogadro's number multiplied by the Boltzman Constant, T is the temperature of the gas, and M is the molar mass of gas [3]. The ratio of specific heats depends on the atomic configuration of the gas,

$$\begin{aligned} \gamma_s &= 5/3 \quad \text{for a monoatomic gas} \\ &= 7/5 \quad \text{for a diatomic gas or linear polyatomic gas} \\ &= 4/3 \quad \text{for a nonlinear polyatomic gas} \end{aligned} \tag{2.2}$$

For Equations 2.1 and 2.2 to hold, three assumptions of the gas must be fulfilled [2]. Firstly, the molecular rotational degrees of freedom must be fully excited and the vibrational degrees of freedom are fully unexcited. This implies that there are no other internal contributions to the specific heat. Secondly, the gas must behave as an ideal gas, whose state is governed by the ideal gas law:

$$P = \rho RT$$

where P is the gas pressure, and ρ is the molar density of the gas. Finally, propagation through the gas must be lossless. Accordingly, there must be no dissipative processes taking place, including thermoviscous transport, molecular relaxation, or chemical reactions.

2.1.1 Corrections to the Laplace formula

The assumptions outlined are a very strict simplification of the system. If the assumptions hold, then the gas is a *simple gas.* If the first assumption is violated, then the gas is an *ideal gas.* If the second assumption is violated then the gas is a *lossless real gas.* This is the case when considering the effects of Van der Wall attraction in the gas. If all assumptions are violated then the gas is a *real gas.* For a real gas, three corrections must be introduced to the Laplace formula for it to hold: specific

heat, virial, and relaxation corrections. Denoting the corrections by the subscripts c, v, and r, respectively, the speed of sound becomes

$$W^2 = \frac{\gamma_s RT}{M}(1 + K_c)(1 + K_v)(1 + K_r) \tag{2.3}$$

where K represents the corrections. To denote quantities of a real gas no subscript will be used, for simple gasses an s will be used, for an ideal gas o will be used, while for a lossless real gas a θ will be used.

2.1.2 Specific heat correction

The specific heat of a real gas is a function of temperature, pressure, and frequency [2]. Following Zuckerwar, the pressure dependence can be drawn into the viral correction and the frequency into the relaxation correction, leaving K_c a function of the specific heat of an idea gas, C_P^o, which is only a function of temperature. The specific heat equation entering into the speed of sound is then

$$\gamma_o = \gamma_o(T) = \frac{C_P^o}{C_V^o} = \frac{C_P^o}{C_P^o - R} = 1 + (C_{oP}/R - 1)^{-1}$$

where

$$\gamma_o = \gamma_s(1 + K_c).$$

If C_P^o is expanded as a power series in temperature T, then

$$C_P^o = a_o + a_1 T + a_2 T^2 + a_3 T^3 + a_{-1} T^{-1}$$

and the correction becomes

$$K_c = (\gamma_o/\gamma_s) - 1 = \gamma_s^{-1}(1 + (a_o - 1 + a_1 T + a_2 T^2 + a_3 T^3 + a_{-1} T^{-1})^{-1}) - 1.$$

The coefficients of C_P^o, along with temperature range under which they are valid can be found in Table 2.1.

Table 2.1: Simple specific heat ratios, coefficients, and valid temperature ranges. Adapted from [4].

Gas	γ_s	a_o	$a_1 \times 10^{-3}$	$a_2 \times 10^{-6}$	$a_3 \times 10^{-9}$	$a_{-1} \times 10^{-9}$	Temp. range (K)
Ar	5/3	1.5	0	0	0	0	10 – 6000
Xe	5/3	1.5	0	0	0	0	10 – 5200
CO_2	7/5	1.35	8.04	−6.72	1.84	0	200 – 590

2.1.3 Virial correction

The viral correction, K_v, is a function of temperature and pressure. The virial equation of state is used since it accounts for attractions between gas atoms. The viral equation is the result of a power series expansion of the molar volume V,

$$\frac{PV}{RT} = 1 + \frac{B}{V} + \frac{C}{V^2} + \dots$$

here B and C are called the second and third virial coefficients, respectively. Higher order terms can be neglected since at high pressures, where the higher order terms would dominate, the state cannot be properly represented as a power series [5]. The real sound speed can then be modeled as

$$W^2 = \frac{\gamma_o RT}{M}(1 + \frac{K}{V} + \frac{L}{V^2} + \dots)$$

where K and L are the results of a three parameter formula and a five parameter formula, respectively, given by Kaye and Laby [2]. The constant K is given by

$$K = a_v(0) + (a_v(1) + \frac{a_v(2)}{T} + \frac{a_v(3)}{T^2}) \exp(c_v/T)$$

where

$$a_v(0) = 2a_v$$

$$a_v(1) = -2b_v$$

$$a_v(2) = \frac{2(\gamma_o - 1)b_v c_v}{\gamma_o}$$

$$a_v(3) = -\frac{(\gamma_o - 1)^2 b_v c_v^2}{\gamma_o}$$

where a_v, b_v, and c_v are experimentally fit parameters [6]. The parameters for Ar, Xe, and CO_2 can be found in Table 4.6. The constant L is given by

$$\begin{aligned} L =& [a_w(0) + a_w(1)\exp(c_v/T) + a_w(2)T^{-2}\exp(c_v/T)]^2 \\ &+ [a_w(3) + a_w(4)T + a_w(5)T^2]\exp(-g_v T) \\ &+ [a_w(6) + a_w(7)T^{-1} + a_w(8)T + a_w(9)T^{-2} + a_w(10)T^2]\exp(f_v/T - g_v T) \\ &+ a_w(11) \end{aligned}$$

where [7],

$$\begin{aligned} a_w(0) &= a_v(1 - \gamma_o^{-1})^{1/2} \\ a_w(1) &= -b_v(1 - \gamma_o^{-1})^{1/2} \\ a_w(2) &= -b_v c_v^2(\gamma_o - 1)(1 - \gamma_o^{-1})^{1/2} \\ a_w(3) &= d_v(2\gamma_o + 1)/\gamma_o \\ a_w(4) &= -d_v g_v(\gamma_o - 1)^2/\gamma_o \\ a_w(5) &= \frac{d_v g_v^2(\gamma_o - 1)^2}{2\gamma_o} \\ a_w(6) &= -e_v[\frac{1 + 2\gamma_o + (\gamma_o - 1)^2 f_v g_v}{\gamma_o}] \\ a_w(7) &= 2e_v f_v(\gamma_o - 1)/\gamma_o \\ a_w(8) &= e_v g_v(\gamma_o^2 - 1)/\gamma_o \\ a_w(9) &= \frac{e_v f_v^2(\gamma_o - 1)^2}{2\gamma_o} \\ a_w(10) &= \frac{e_v g_v^2(\gamma_o - 1)^2}{2\gamma_o} \\ a_w(11) &= c_\infty(1 + 2\gamma_o)/\gamma_o \end{aligned}$$

The virial correction can then be written as

$$K_v = \frac{P}{RT}K + (\frac{P}{RT})^2(-BK + L)$$

where B is

$$B = a_v - b_v \exp(c_v/T)$$

The coefficients for L can be found in Table 2.3.

Table 2.2: Values for constants of the Second Virial coefficients with valid temperature ranges. Adapted from [8].

Gas	a_v (cm^3/mol)	b_v (cm^3/mol)	c_v (K)	Temp. range (K)
Ar	154.2	119.3	105.1	$80 - 1300$
Xe	245.6	190.9	200.2	$160 - 650$
CO_2	137.6	87.7	325.7	$220 - 1100$

Table 2.3: Values for constants of the Third Virial coefficients with valid temperature ranges. d_v, e_v, and c_∞ have units of (cm^3/mol), while f_v has (K), and g_v has units of (K^{-1}). Adapted from [8].

Gas	d_v	e_v	f_v	g_v	c_∞	Temp. range (K)
Ar	13439.72	2304.823	146.3464	0.01	761.25	$80 - 1223$
Xe	58442.23	602.336	992.313	0.008	1829.25	$209 - 573$
CO_2	113548.2	83.43604	1581.725	0.011	1556.2	$230 - 773$

2.1.4 Relaxation Correction

The final correction to the Laplace equation is the relaxation correction, K_r. The relaxation correction is a function of temperature, pressure, and frequency. The correction is a representation of the dissipative processes in a gas. As a wave propagates through a gas it disturbs all of the degrees of freedom of the constituent molecules, not just the translational equilibrium. The disturbance is then propagated by molecular collisions in the gas. Relaxation is the process where by the gas returns to equilibrium. Since relaxation is transmitted through collisions the time delay between collisions causes dispersion of the sound wave which is where the frequency dependence arises. Relaxation can be treated as either a single relaxation process, where the molecular excitation is characterized by a single process; or multiple relaxation processes, where the molecular excitation is characterized by multiple simultaneous reactions. To first order any multiple relaxation process can be given by a single relaxation process.

The relaxation process is characterized by two parameters, the relaxation strength, ϵ, and the relaxation time, τ. The relaxation process is characterized by two different relaxation times, the time related to dispersion and the time related to sound absorption. The dispersion term accounts for the frequency dependence of sound speed and is related by the following;

$$W^2 = W_\theta^2[1 + \frac{\epsilon}{\sqrt{1-\epsilon}}\frac{(\omega\tau)^2}{1+(\omega\tau)^2}] \tag{2.5}$$

where W_θ is the sound speed in the limit of zero frequency with virial and specific heat corrections, and where $\omega = 2\pi f$ is the angular frequency of the wave [9]. From Equation 2.5 the relaxation correction K_r is given by

$$K_r = \frac{\epsilon}{\sqrt{1-\epsilon}}\frac{(\omega\tau)^2}{1+(\omega\tau)^2} \ . \tag{2.6}$$

The relaxation strength is determined by examining the high frequency limit of Equation 2.5. In this limit the sound speed approaches the limit

$$W_\infty = \frac{W_\theta}{\sqrt{1-\epsilon}}$$

which can be rearranged to give

$$\epsilon = 1 - \frac{W_\theta^2}{W_\infty^2}.$$

The relaxation strength by definition is the the fractional difference between isentropic compressabilities,

$$\epsilon = \frac{\kappa_S^\theta - \kappa_\theta^\infty}{\kappa_S^\theta}$$

which can be expressed in terms of specific heats as

$$\epsilon = \frac{RC_i}{(C_P^o - C_i)(C_P^o - R)}$$

where $C_i = C_V^\theta - C_V^\infty$, the difference between the low frequency and high frequency

specific heats or the specific heat of the relaxing degree of freedom. The rotational degree of freedom is given by

$$\begin{aligned} C_i &= R \text{ for a linear molecules} \\ &= \frac{3}{2}R \text{ for nonlinear molecules} \end{aligned}$$

while the ith mode of the vibration degree of freedom is

$$C_i = q_i R(\frac{\theta_{vb}^{(i)}}{T})^2 \frac{\exp(-\frac{\theta_{vb}^{(i)}}{T})}{[1-\exp(-\frac{\theta_{vb}^{(i)}}{T})]^2}. \tag{2.7}$$

where θ_{vb} is the vibrational temperature.

The relaxation time is given by Schwartz, Slawsky, and Herzfeld (SSH Theory) as:

$$\log(\tau P) = a_r(1) + a_r(2)T^{-1/3} + a_r(3)T^{-1}$$

where τ is expressed in microseconds and P is expressed in atm [3]. The values for $a_r(i)$ along with the vibrational temperature can be found in [10].

2.2 Mixing

In the case of multiple gasses, the parameters of the corrections change. This change is dependent on both the individual properties of the gas, as well as its fraction of the whole mixture. This thesis is only concerned with the mixing rules for CO_2 with a monoatomic gas, like Ar and Xe. Since monoatomic gasses do not have vibrational degrees of freedom they do not have specific heat or relaxation corrections. Therefore, the specific heat correction and the relaxation correction will only be dependent on the CO_2 and the percentage of the mixture it makes up. As a result two new quantities become important to the Laplace formula, denote the fraction of CO_2 as x and the mass of the monoatomic gas as M_m.

Assuming the mixing of gasses, the Laplace formula can be written as

$$W^2 = \frac{\gamma_{s-mix} RT}{M_{mix}}(1 + K_{c-mix})(1 + K_{v-mix})(1 + K_{r-mix})$$

where M_{mix} is merely the molar mass of the mixture, given by

$$M_{mix} = \sum x_i M_i = xM_{CO_2} + (1 - x)M_m.$$

The molar masses of Ar, Xe, and CO_2 are 39.9278 g, 131.29 g, and 44.010 g, respectively. Since the mixtures are between a monoatomic gas and carbon dioxide, the specific heat and relaxation corrections of the mixture will not depend on the monoatomic gas since it does not have vibrational freedom. In general, for a mixture the specific heat is given by

$$\frac{C^o_{pmix}}{R} = \frac{1}{R}[xC^o_{pco2} + (1 - x)C^o_{pm2}] = x\sum_n (a_{n-co2} - a_{n-m})T^n + \sum_n a_{n-m}T^n$$

If $A = \sum_n (a_{n-co2} - a_{n-m})T^n$ and $\sum_n a_{n-m}T^n$ then

$$\gamma_{omix} = \gamma_{smix}(1 + K_c) = 1 + (Ax + B - 1)^{-1}$$

where a_n are the coefficients for the pure gases [11].

Unlike the specific heat correction, which is independent of the other gases in the system, the viral correction, which accounts for attractions between the gas atoms, has a cross term. In a two gas mixture the second viral coefficient is

$$K_{mix} = x^2 K_{11} + 2x(1 - x)K_{12} + (1 - x)^2 K_{22}$$

where K_{11} and K_{22} are the second viral coefficient of the pure components. The cross term, $K_{12} = E + (K_{11} + K_{22})/2$, where E is the excess second virial coefficient at the specific temperature of the mixture [12]; however, this term is negligibly small compared to the pure second viral coefficients and can be ignored [13]. Since the

third virial coefficient accounts for second order attractions there are four terms,

$$L_{mix} = x^3 L_{111} + 3x^2(1-x)L_{112} + 3x(1-x)^2 L_{122} + (1-x)^3 L_{222}$$

where L_{111} and L_{222} are the pure third virial coefficients, $L_{112} = (L_{111}^2 L_{222})^{1/3}$, and where $L_{112} = (L_{111} L_{222}^2)^{1/3}$. The virial correction for the mixture is of the same form as for a single gas, but where K and L are replaced with K_{mix} and L_{mix}. Since monoatomic gases do not have vibrational modes of freedom, only CO_2 contributes to the relaxation correction. The relaxation strength is given by

$$\epsilon = \frac{RxC_{ico2}}{(C^o_{pmix} - xC_{ico2})(C^o_{pmix} - R)}$$

with

$$C^o_{pmix} = xC^o_{pco2} + (1-x)C^o_{pm}$$

where C^o_{pco2} and C^o_{pm} are $7/2R$ and $3/2R$, respectively [14]. The specific heat for the rotational degrees of freedom are given by Equation 2.7, where θ_{vb} is 959.7 K. Even though the monoatomic gas does not contribute to the relaxation strength it does contribute to the relaxation time. The relaxation time is thus given by

$$\frac{1}{\tau} = \frac{x}{\tau_{co2}} + \frac{1-x}{\tau_{co2-m}}$$

where τ_{co2} is the relaxation time of one CO_2 molecule in pure CO_2 gas, and τ_{co2-m} is the relaxation time of one CO_2 molecule in the pure monoatomic gas. The relaxation correction is then given by Equation 2.6,

$$K_r = \frac{\epsilon}{\sqrt{1-\epsilon}} \frac{(\omega\tau)^2}{1+(\omega\tau)^2}.$$

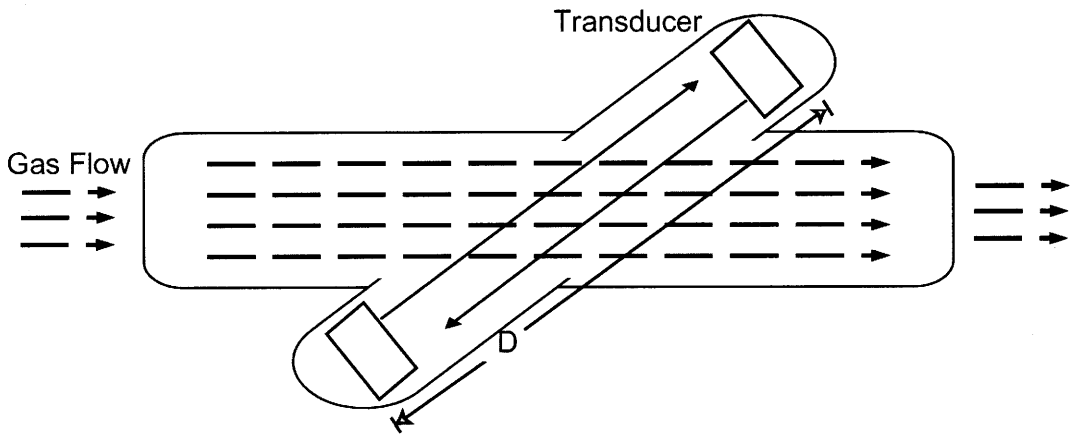

Figure 2-1: Schematic of how to measure sound speed. The dotted lines represent a flowing gas with velocity v, while the solid lines represent sound pulses that in the absence of gas flow, travel with the speed of sound.

2.3 Composition Measurement Using Sound Transit Time

In the previous section the velocity of sound was derived for a real gas and for a mixture of real gases. The derivation assumed that the net motion of the gas, the sum of the velocities of the individual molecules, was zero. If the gas is flowing then the speed of sound is given by

$$W_{flow} = W + v.$$

where W is the real speed of sound if there is no flow, and where v is the net velocity of the gas. Similarly, the observed frequency of the speed of sound is given by the Doppler Shift,

$$\omega_{lab} = \omega_{emit} \frac{W}{W - v}.$$

where ω_{emit} is the emitted frequency. The time it takes for the wave to transverse a distance D is thus

$$tt = D/W_{flow}$$

where tt is referred to as the transit time. If a wave pulse was produced and passed through a region of gas flow that is nearly parallel to the waves direction and was then picked up by a receiver a distance D away, then the transit time is given by

$$tt = D/(W + v)$$

and

$$tt = D/(W - v)$$

for a wave traveling against the flow of the gas. The speed of sound of the still gas is then

$$W = \frac{D}{2}\frac{(tt_1 + tt_2)}{tt_1 tt_2}$$

where tt_i are the transit times in the two directions. In the case where $tt_1 \sim tt_2 = tt$ this reduces to

$$W = \frac{D}{tt}$$

and the for a real gas the transit time is then

$$tt = \sqrt{\frac{M}{\gamma_s RTD(1 + K_c)(1 + K_v)(1 + K_r)}}\,. \tag{2.8}$$

Chapter 3

Experiment

The main aim of this thesis is to determine the feasibility of using a ndd Medizintechnik Spiroson-AS spirometer to determine the composition of a gas in AMS02. The spirometer will be integrated into the gas circulation box (Box-C) of the TRD where the gas is supplied to the manifolds that distribute the gas throughout the TRD module. Since this thesis is concerned with the integration of the spirometer on AMS, to simulate this environment, the spirometer was placed in an airtight box. The measured gas mixture was supplied to the sealed box via a regulator. Using a flow meter the gas was flowed through the box for 10 minutes to ensure that the box only contained the gas to be tested. Attached to the inlet gas feed inside the box was a three inch long piece of tubing with holes in it, to help evenly disperse the gas inside the box. Connected to the gas inlet and outlet of the box were needle valves, which were used to seal the box, outlet valve first. The box consisted of a Spirometer and four Dallas DS18S20 Temperature sensors. This chapter examines the setup for measuring transit times using a spirometer.

3.1 Spirometer

The spirometer is a high precision pressure transducer. The spirometer consists of an open ended cylindrical tube which intersects an oblique cylindrical channel. Mounted at the opposite ends of the channel are a pair of transducers composed of a microphone

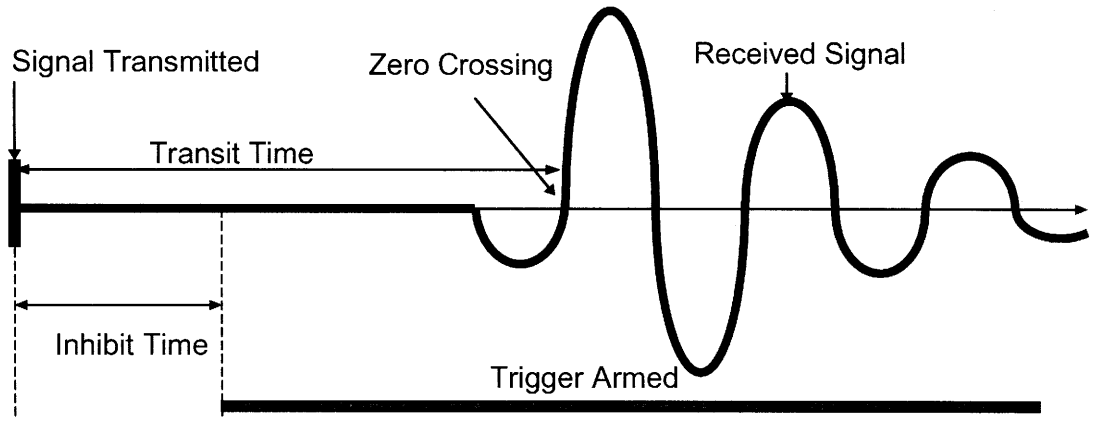

Figure 3-1: Spirometer transit time measurement. Adapted from [16].

and loudspeaker. At short user defined intervals, one two-hundredth of a second was used for this experiment, ultrasonic pulses are emitted by the loudspeakers and are picked up by the opposite microphone as explained in Section 2.3 and depicted in Figure 2-1. The pulse picked up in the opposite microphone is then converted back into an electrical pulse that is used to measure the transit time.

The spirometer is controlled by an application-specific-integrated-circuit (ASIC A1), which is what actually calculates the transit time. The ASIC sends a 1.25 V $\pm$0.1 V square wave pulse of 100 MHz to the microphone where it is converted to an ultrasonic pulse [16]. The imperfect nature of the transducers distorts the square pulse into a sinusoidal pulse. The time when the pulse is emitted is referred to as the time of transmission. The entire transit time measurement is depicted in Figure 3-1. When the pulse is picked up by the opposite microphone, the signal is converted back to an electrical signal where it is received by the ASIC. The transit time is the time between the ASIC sending the signal to the loudspeaker and receiving the picked up signal from the opposite microphone. The transit time is measured from the first zero crossing of the received signal as the exact time between the time of transmission (or Signal transmission time) and the time of the zero crossing. Since interference, self triggering, and other electronic and acoustic problems could lead to improper measurements, the trigger for the zero crossing is only armed at specific

times. Immediately after transmission the trigger is unarmed for a programmed amount of time referred to as the inhibit time. For this experiment the inhibit time was 100 μs, so any signals received by the microphone prior to 100 μs are ignored. The transit time recorded by the ASCI is then sent to an External EEPROM Logic Converter where it is sent to the serial port of the computer and recorded using a LabView interface. (The resulting up- and down-stream transit times are determined to a resolution of 10 ns. For the following experiments, 200 transit time samples were taken every second and averaged.)

3.2 Temperature Sensors

The goal of this thesis is to accurately calibrate the spirometer, as a result the temperature must be known to a high degree of precision. According to the theoretical prediction, the transit time increases linearly with increasing temperature at a rate of 0.31 μsec/C. Since the spirometer is accurate to 10 ns, the spirometer is sensitive to a temperature change of 0.1 C. Attached to the ends of the flow tube are four Dallas DS18S20 Digital Thermometers. These temperature sensors measure the temperature of the gas as it passes through the spirometer. The DS18S20 provides a 9-bit centigrade temperature measurement which gives a resolution of one fifteenth of a degree Celsius. What is unique about the DS18S20 is that it derives its power directly from the data line while communicating over a 1-Wire bus which allows for multiple temperature sensors to be read by a single microprocessor. The sensors are controlled by the DS18S20 Temperature Reader (DSTR). The DSTR is an ASCI composed of a PIC16F628 microcontroller and a MAX233CP. Each DS18S20 has a unique 64 bit identification code, which it sends along with its temperature reading. The PIC converts the hexadecimal encoded temperature to a string of ASCII character which it then sends to the serial port of the computer where it is recorded using a LabView interface.

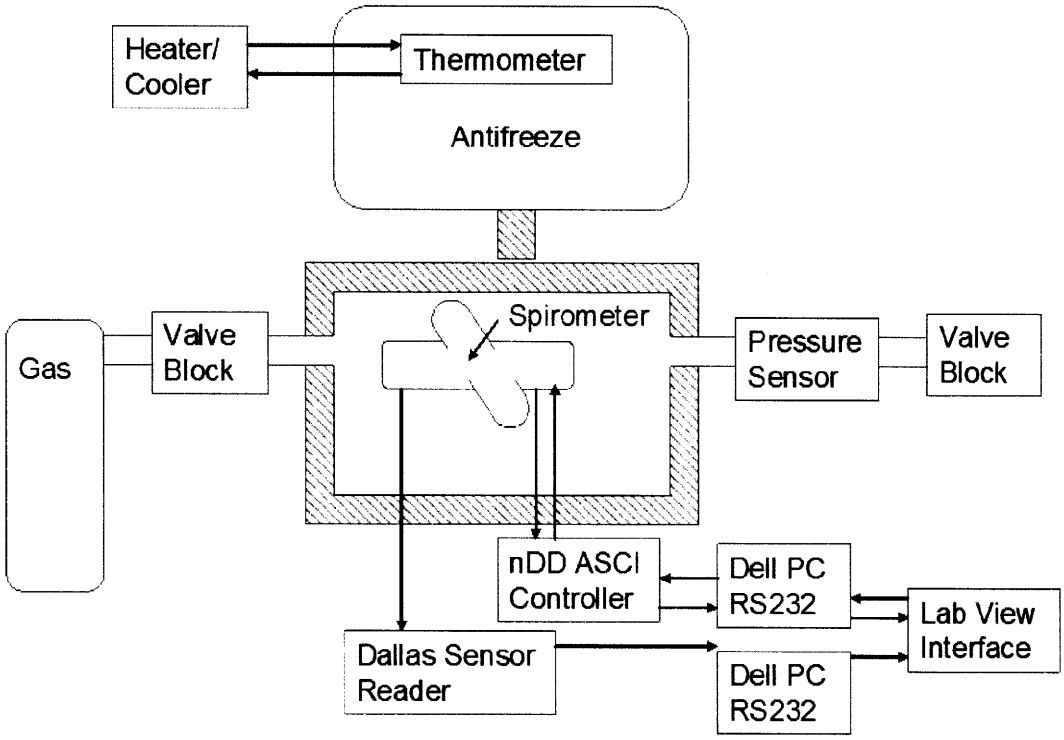

Figure 3-2: Transit time experiment setup

3.3 Experimental Setup

The apparatus consisted of a spirometer, an Omega digital pressure sensor, a Freon refrigeration coil and an aquarium heater, four Dallas DS18S20 temperature sensors, and the DSRT. A depiction of the apparatus can be found in Figure 3-2. Since the spirometer needed to be isolated from laboratory temperature and pressure conditions, the spirometer was placed in a stainless steel box which was sealed with an o-ring. This box was further insulated by a one inch thick layer of Styrofoam core. Thermally coupled to the stainless steel bath was a 7.56 L bath of antifreeze. The Freon refrigeration coil and the aquarium heater were submerged in the antifreeze to modulate the temperature of the bath. The combination of the two heating elements could modulate the temperature of the container from -2 C to 32 C.

For the measurement of the transit time of a mixture of gas, the gas was first passed through a flow-meter where its flow rate could be monitored and modulated.

Using the flow meter the gas was flowed through the box for 30 minutes to remove any trapped gases from previous trials. Attached to the gas inlet inside the stainless steel box was a three inch long piece of tubing with holes in it, to help evenly disperse the gas inside the box. Connected to the gas inlet and outlet outside of the box was a pair needle-valves and an Omega pressure sensor. Once the gas had circulated throughout the box the bath was brought to a temperature of 30 C by the aquarium heater. The valves were then closed, trapping the gas inside the box at a pressure of approximately 1.03 bar. The system was then allowed to equilibrate for five minutes to ensure the gas was the same temperature of the box. Using the LabView program the activate command was sent to the spirometer ASCI A1. When active the spirometer continuously measured the transit time. The transit time was measured by the spirometer 100 times and averaged. With a sample rate of 200 Hz the spirometer was active for approximately one half of a second. The stop command was then sent to the spirometer and the temperature was measured by the temperature sensors. Using a Freon refrigeration coil the bath could be cooled to a temperature of -20 C. Using a timer that controlled the power sent to the coil, the temperature of the gas was modulated from 0°C - 30°C. By recording the transit time of the gas as it was cooled then warmed, the transit times dependence on temperature could be determined. For each trial the gas was brought to 0°C then returned to 30°C which took approximately 8 hours. The transit time as a function of temperature was measured for Ar-CO_2 mixtures of 80 : 20, 85 : 15, 90 : 10, 95 : 5, and 100 : 0. The results for these mixtures can be found in Figure 3-3.

3.4 Spirometer Pressure Dependence

Prior to measuring the transit time's dependence on temperature, the stability of the spirometer's measurement ability was checked at different pressures for the same temperature. According to Equation 2.6, the speed of sound should not depend on pressure, so at a constant temperature any changes in the transit time would be due to hardware limitations of the spirometer. The spirometer was attached to a pressure

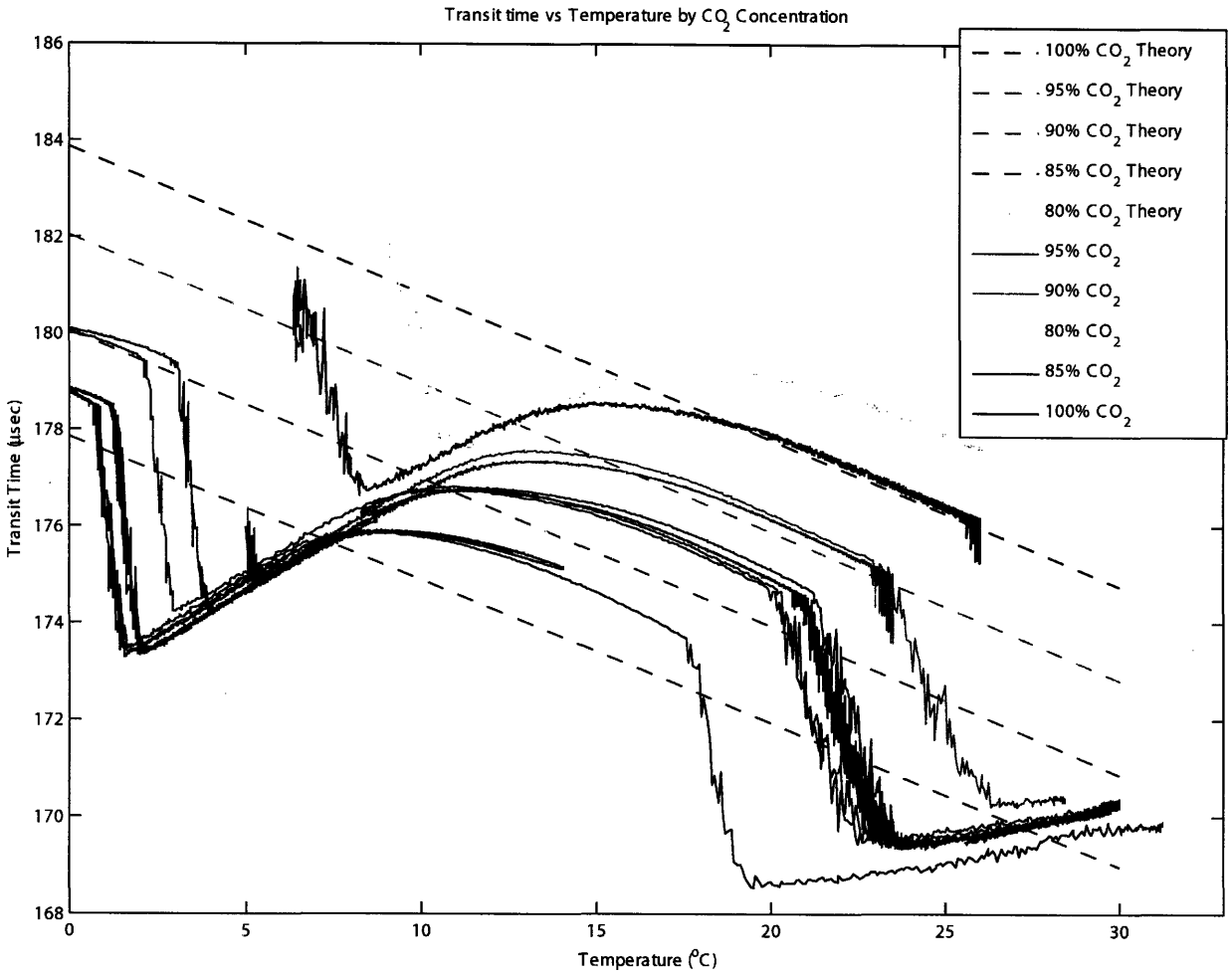

Figure 3-3: A plot of transit time dependence on temperature for a series of Ar CO_2 mixtures. The gas was trapped in the stainless steel box and then the temperature was modulated using the antifreeze bath. The dotted lines represent the theoretical predictions while the solid lines are the recoded data from the LabView interface.

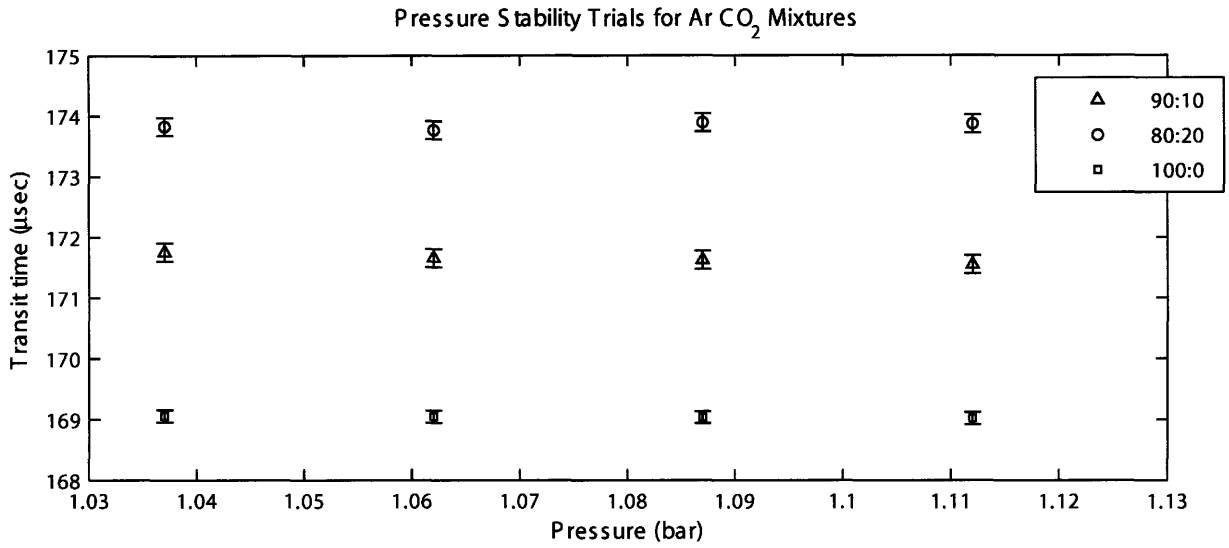

Figure 3-4: Pressure dependence on Transit Time measurements in the spirometer.

column to determine the stability for measurements. The pressure column consisted of a 1.25 m glass tube filled with water and closed at both ends. The column contained a series of tubes which were fed through the top of the column and terminated at different depths inside the column. By attaching the apparatus to these different tubes, the pressure of the system could be changed to 1.037, 1.062, 1.087, and 1.112 bar. Gas was slowly flowed through the apparatus at room temperature while the spirometer was activated. The stability was checked for 80 : 20, 90 : 10, and 100 : 0 since they were the minimum, middle, and maximum mixtures that would be used to calibrate the spirometer. The transit time of each gas was measured at each of the four pressures. The results can be found in Figure 3-4 and are discussed in section 4.1.

Chapter 4

Analysis

Given the speed of sound in a real gas,

$$W^2 = \frac{\gamma_s RT}{M}(1 + K_c)(1 + K_v)(1 + K_r) \tag{4.1}$$

which is comprised of a mixture of CO_2 and Ar, the transit time can be written as a quadratic function in terms of CO_2 concentration, i.e.

$$tt(T) = a_o(T) + a_1(T)x + a_2(T)x^2 \tag{4.2}$$

By measuring the transit times for Ar CO_2 mixtures of 100 : 0, 95 : 5, 90 : 10, 85 : 15, and 80 : 20, the values for a_o, a_1, and a_2 can be determined for different temperatures. Once these coefficients are determined, the concentration of any Ar CO_2 mixture can be determined using the coefficients, the temperature, and the transit time. This section will address how to determine these coefficients along with the sources of error for the experiment.

4.1 Pressure Dependence Results

Using a pressure column the transit time was measured at 23.5 ^oC for mixtures of Ar CO_2 100 : 0, 90 : 10, and 80 : 20. For each trial the transit time for the specific mixture

was measured for ten minutes at a given pressure. Each trial was run three times where the mean of the trials was the transit time and the variance in measurement was the standard deviation. The data can be found in Figure 3-4. For each mixture the transit times remained within 0.6σ, which suggests that the spirometer measurement is not affected by pressure. Similarly, the data was fit with a linear regression of the form $tt = a_1 * x + a_2$. The slopes of the fits, a_1, is within two σ of zero for each mixture. Furthermore, the fits all shared R^2 values that were approximately 0.70, which suggests the data is not linear, but rather a constant value. Therefore, these results suggest when measuring the temperature dependence, the pressure of the trial should not be a factor and can be neglected as long as it is approximately 1 bar ± 0.112 bar.

Table 4.1: Coefficients for linear fit of transit time as a function of pressure for different the Ar CO_2 mixtures plotted in Figure 3-4.

	100:0	90:10	80:20
a_1	-0.47 ± 0.21	-2.5 ± 1.5	1.0 ± 4.1
a_2	169.6 ± 0.3	174.4 ± 1.6	172.7 ± 4.6

4.2 Temperature Dependence Results

After finding the spirometer to be unaffected by pressure, the transit time's temperature dependence was analyzed. The transit time for each gas mixture was measured following the procedure of Section 3.4. There were at least four independent trials per gas where fresh gas was flowed through the box and then sealed. Using a simple script, the transit times for these trials were averaged over the resolution of the Dallas sensors to give an average transit time for each temperature. The results are plotted in Figure 3-3 for all measured mixtures of Ar CO_2.

4.2.1 Determining the CO_2 concentration

In the spirometer, the speed of sound is the amount of time it takes for the sound pulse to transverse the flow tube to its counter's receiver. If the distance between speaker is known, which it is in the specifications and verified through measurement, then the corrected Laplace equation can be inverted to yield the transit time as a function of temperature, i.e,

$$tt = \sqrt{\frac{M}{\gamma_s RTD(1+K_c)(1+K_v)(1+K_r)}} \tag{4.3}$$

where D is the distance between speaker and receiver. Since M, K_c, K_v, and K_r all depend on the CO_2 concentration, the temperature can be held constant and the CO_2 concentration can be varied. The resulting plots of transit time as a function of CO_2 concentration can be found in Figure 4-1. By observation of the curves, expanding the transit time as a power series in x, the fraction CO_2, all terms of cubic or higher may be ignored. This results in a transit time of the form

$$tt(T) = a_o(T) + a_1(T)x + a_2(T)x^2 \tag{4.4}$$

where a_o, a_1, and a_2 are temperature dependent functions.

Using a simple matlab script, the experimental transit time was determined as a function of CO_2 concentration. When given a temperature, the script would take all the trials for that specific gas and average their transit times that were within two fifteenths of the temperature. The standard deviation of this mean was used as the error in the measurement. The transit time as a function of CO_2 was measured at 25 C, 20 C, 15 C, and 10 C and can be found in Figure 4-2 through Figure 4-5. From the figures it is clear that for the temperature range 15C-25C the CO_2 concentration can be measured to within 2%. For higher temperatures (those between 25 C and 20 C) mixtures with a concentration of CO_2 greater than 0.1 agree with theory, while for lower temperatures ($15 - 10$ C) concentrations below 0.1 tend to agree with data. The nature of the agreement is a result of the unexpected drops in the transit time

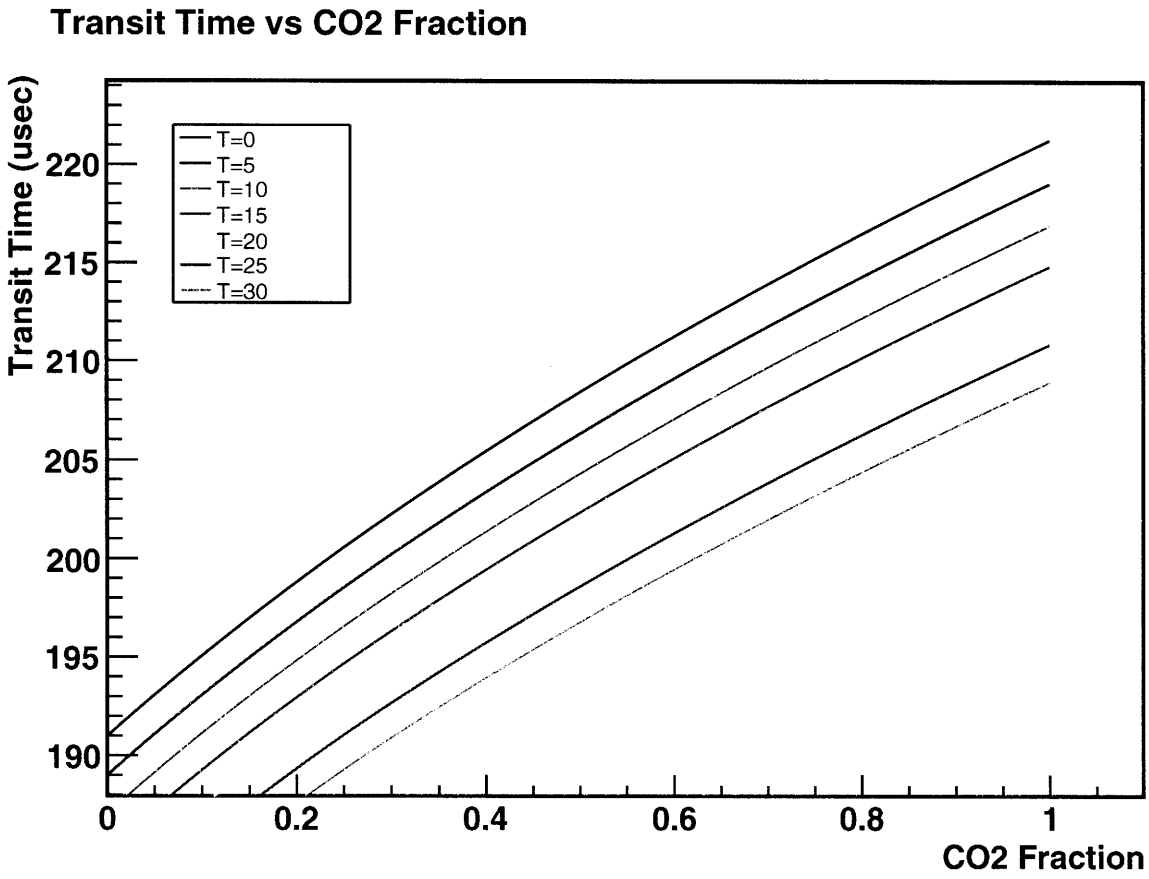

Figure 4-1: Transit time as a function of CO_2 fraction for different temperatures.

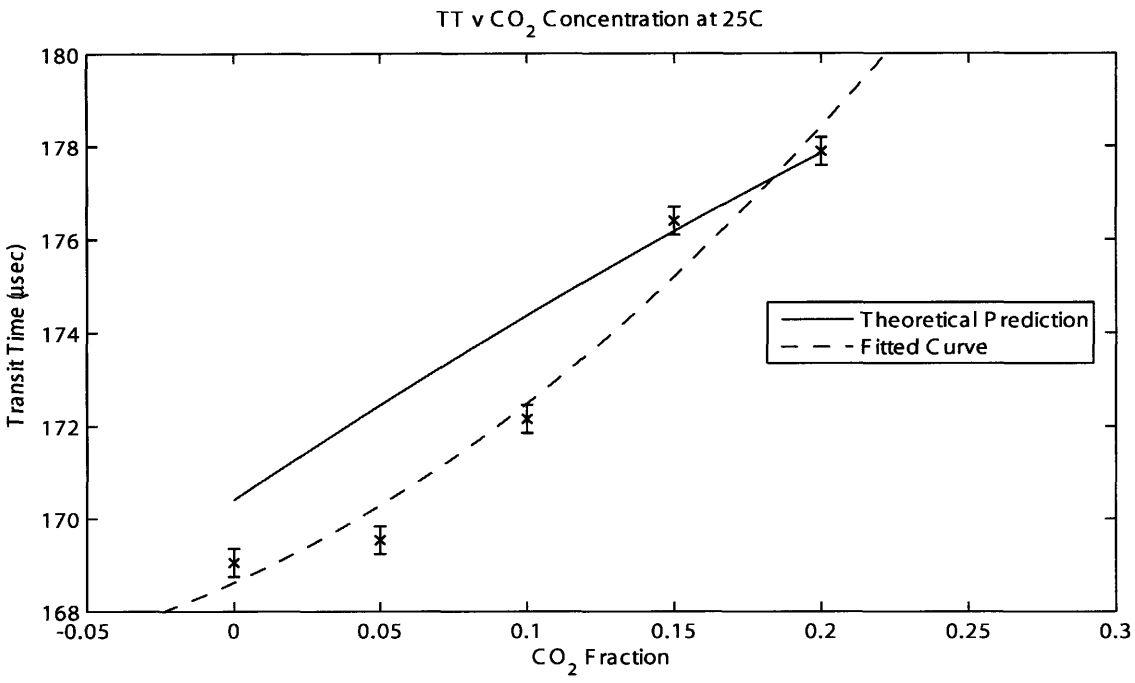

Figure 4-2: Transit time as a function of CO_2 fraction for 25 C.

curves, which are discussed in Section 4.2.3.

4.2.2 Unusual behavior in temperature dependence

As suggested in Equation 2.8, the transit time should have an approximate linear dependence on temperature between 0 C and 30 C, decreasing with increasing temperature at a rate of 0.31 μsec/C; however in the experimental data there are a points where the transit time drops at a much quicker rate, then increases. These dips were reproducible, and to a degree predictable. The nadir of the dips was dependent on the CO_2 fraction, and were determined by fitting lines to the two legs of the dip. Fitting a linear regression to the nadir of the lower dip (the dip occurring between 0 C and 12 C) and the temperature at which it occurred for 100:0, 95:5, 90:10, and 85:15 accurately predicted the position of the nadir of 80:20 to 0.3 C. It is believed that these dips are the results of hardware limitations. A series of tests were run in order to determine the cause of these dips. The first test was to determine if the dip was the result of a resonance in the flow tube; one end of the tube was covered

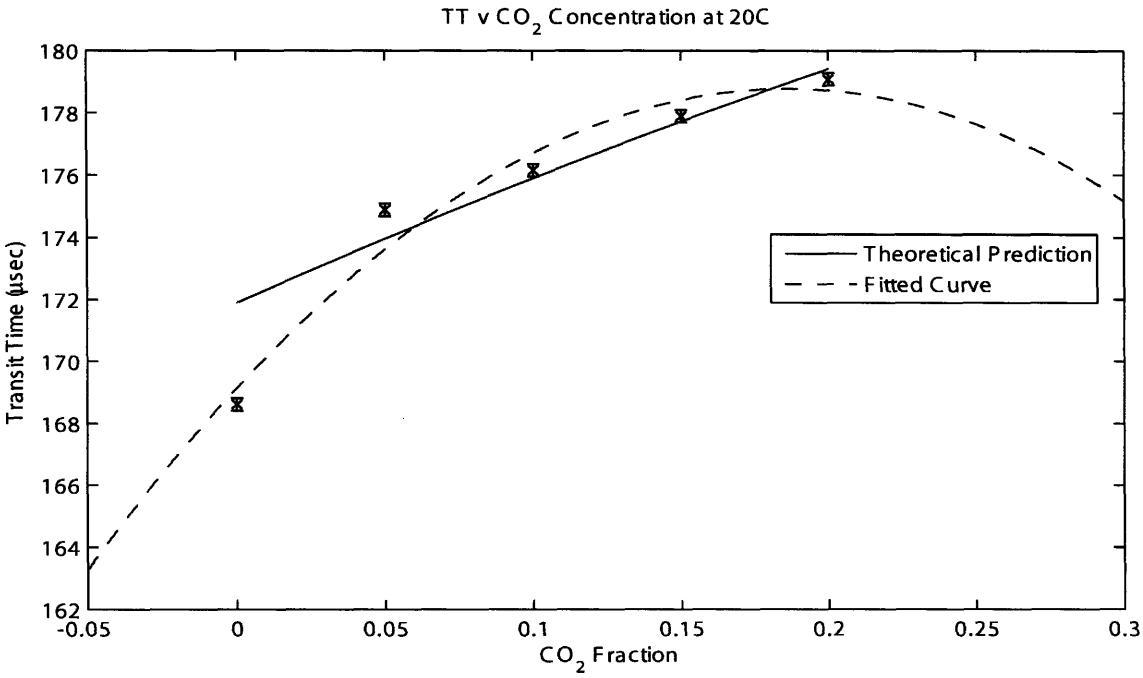

Figure 4-3: Transit time as a function of CO_2 fraction for 20 C.

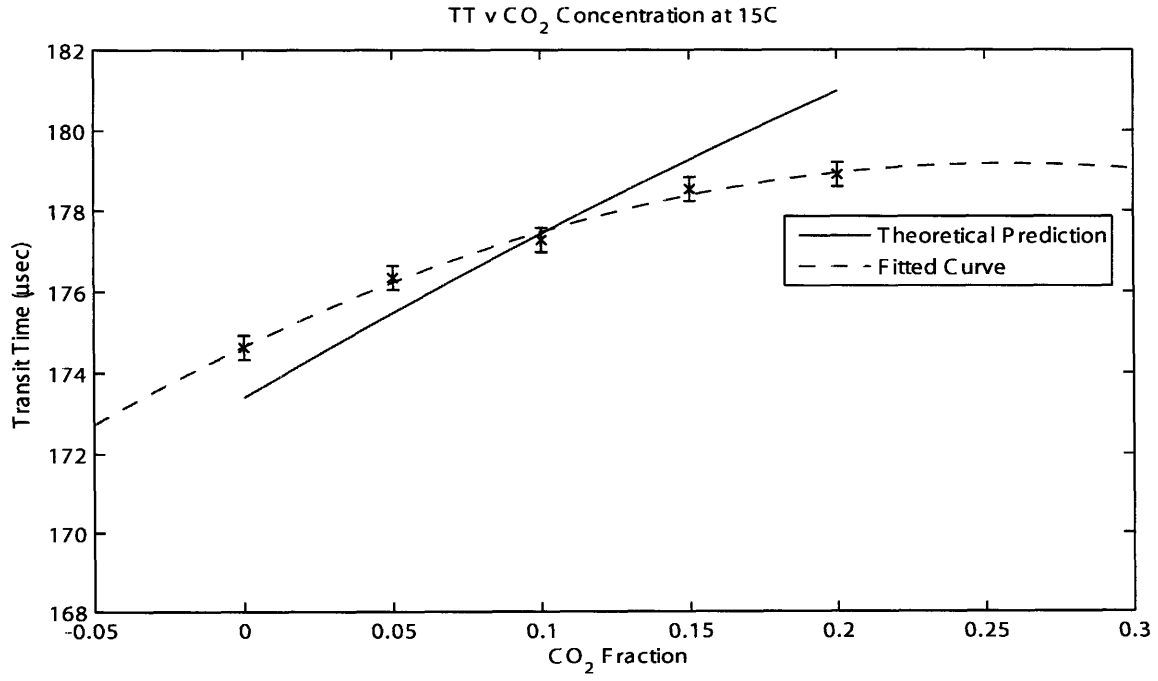

Figure 4-4: Transit time as a function of CO_2 fraction for 15 C.

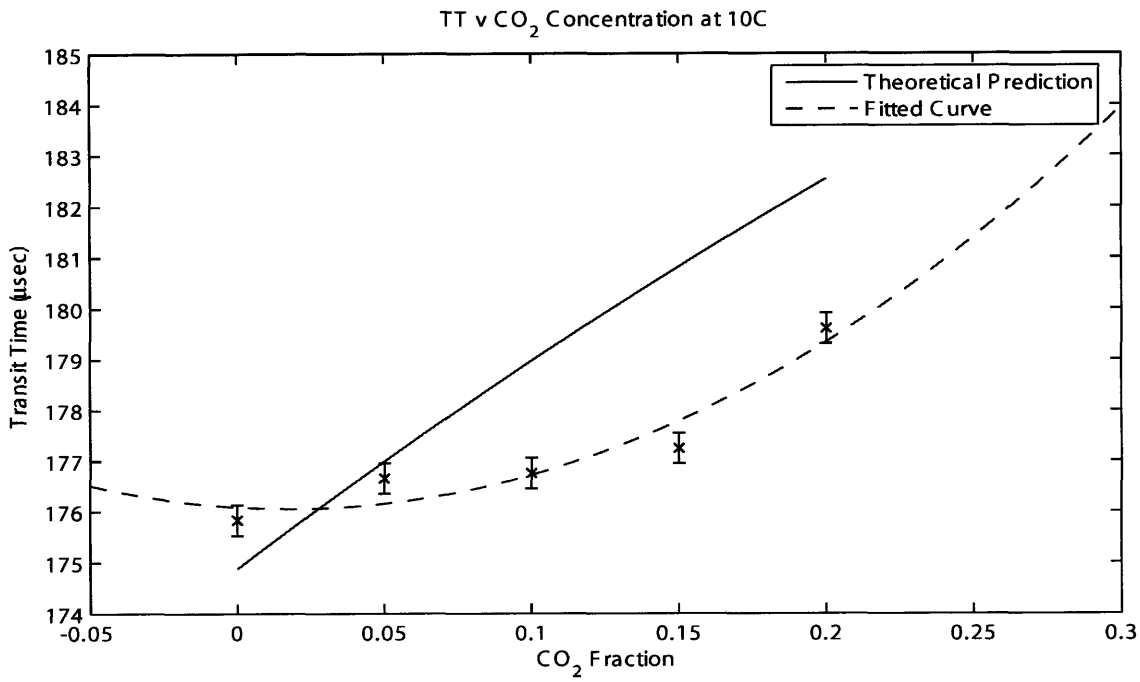

Figure 4-5: Transit time as a function of CO_2 fraction for 10 C.

and the experiment was run again for 100:0. This was found to have a negligible effect on the relative position of the dip. Similarly, the experiment was run with the spirometer's power supply at 5.5 V rather than 9 V. This too was found to have a negligible effect.

If a continuous function could be determined to describe the shape of the temperature curves, then the dependence of those parameters on CO_2 concentration and temperature could be determined. Using this function as the calibration rather than the theoretical curves would lead to a more accurate prediction of the CO_2 concentration. Since the shape of the transit time curves is the same for the mixtures, if each of the transit time curves were fit using this continuous function, then the parameters of the function could be plotted for the mixtures as a function of CO_2 concentration. From this plot the parameters dependence on concentration could be evaluated.

4.2.3 Temperature fits

For the spirometer to be used on AMS02, a functional form of the transit time versus the CO_2 concentration must be determined for different temperatures. The data's agreement with the theoretical predictions has already been discussed. Aside from the theoretically predicted curves, each set was fit with the quadratic polynomial suggested by Equation 4.2, to more accurately describe the data. These fitted curves can be found in Figure 4-2 through Figure 4-5. The fit parameters can be found in Table 4.2.

Table 4.2: Coefficients for quadratic fit of transit time as a function of CO_2 fraction at different temperatures.

	10 C	15 C	20 C	25 C
a_1	99 ± 267	-68 ± 91	-277 ± 523	103 ± 524
a_2	-3 ± 49	35 ± 19	103 ± 109	28 ± 72
a_3	176.1 ± 2.4	174.7 ± 0.8	169.2 ± 4.6	168.6 ± 4.6

Using the fitted curves, the spirometers' ability to determine the composition of a Ar CO_2 gas mixtures can be determined. By taking the minimum and maximum of each transit time measurement, as determined by the error-bars, we can determine what concentrations these extremes would correspond to on the fitted curves. This was performed on the the transit time versus CO_2 concentration graphs and the results can be found in Table 4.3 through Table 4.6. Averaging of the difference between the concentration suggested by the minima (and maxima) and the actual concentrations, the spirometer was found to have the ability to determine the composition of a Ar CO_2 gas mixture to within $1.75\% \pm 1.23\%$.

Table 4.3: Minima and maxima of CO_2 concentrations at 25 C based on the error in transit time measurements.

CO_2 Frac.	0.00	0.05	0.10	0.15	0.20
min	0.0046	0.0205	0.0873	0.1647	0.1876
max	0.0238	0.0375	0.0991	0.1740	0.1965

Table 4.4: Minima and maxima of CO_2 concentrations at 20 C based on the error in transit time measurements.

CO_2 Frac.	0.00	0.05	0.10	0.15	0.20
min	–	0.0633	0.0836	0.1210	0.1863
max	0.0020	0.0725	0.0919	0.1405	–

Table 4.5: Minima and maxima of CO_2 concentrations at 15 C based on the error in transit time measurements.

CO_2 Frac.	0.00	0.05	0.10	0.15	0.20
min	–	0.0436	0.0784	0.1411	0.1701
max	0.0081	0.0652	0.1046	0.1880	–

Table 4.6: Minima and maxima of CO_2 concentrations at 10 C based on the error in transit time measurements.

CO_2 Frac.	0.00	0.05	0.10	0.15	0.20
min	–	0.0771	0.0799	0.1131	0.1988
max	0.0344	0.116	0.1247	0.1436	0.2153

Chapter 5

Conclusion

Following the goal of this thesis, the spirometer was successfully shown to differentiate between mixtures of Ar CO_2. The spirometer was calibrated to determine CO_2 concentration in Argon CO_2 mixtures. The spirometer was successfully able to differentiate between mixtures for temperatures between 15 C and 25 C. Moreover, the spirometer can differentiate between mixtures of 80:20 and 85:15 from 7 C to 25 C, except for between 11 C and 14 C. Using fitted curves, the spirometer was found to have the ability to determine the composition of the Ar CO_2 mixtures to within $1.75\% \pm 1.23\%$. The spirometer was also found to behave independently of pressure, as theoretically predicted, so no pressure corrections are necessary to transit time measurements.

It is clear from Figure 3-3 that the spirometer can detect CO_2 fraction by measurement of the transit time. Due to the presence of dips in the measurement of the transit time as a function of temperature, the agreement of the spirometer results with the theoretical expectations are not consistent for all temperatures. For temperatures between 15 C and 25 C there is a clear difference between 80:20 and 85:15 and they follow the theoretical predictions. The lower concentrations of CO_2 do not follow the theoretical predictions in this regime. For the purposes of AMS02, where the mixtures will be approximately 80:20 this is suitable. Similarly, the spirometer is unable to accurately resolve the differences between certain mixtures between 12 C and 2 C as the result of unexpected dips in the transit times. The exact cause of

this phenomenon is unknown, however, in lieu of finding a continuous function that describes the function, it may be treated piecewise. Treating the curves as piecewise, the theoretical predictions of transit time's dependence on CO_2 concentration were abandoned in favor of quadratic functions, which were fit to the transit time curves at 25 C, 20 C, 15 C, and 10 C and were used to show the spirometer could determine composition to within $1.75\% \pm 1.23\%$.

Since the cause of the dips is unknown, in order to determine if the dips are the result of Ar, CO_2, or a property of the mixture, the temperature dependence of the transit time should be measured for other mixtures of gas, such as Ne Ar or Ne CO_2. Furthermore, since the spirometer has been shown to have the ability to determine the composition of a gas mixture to within $1.75\% \pm 1.23\%$, well within the necessary 3% required for AMS02, the transit time behavior of Xenon must be studied. Since Xenon is three times heavier than Argon there may be differences in the shape of the plots.

Appendix A

Figures

The following figures give a flavor of the size of the corrections for Ar CO_2 mixtures. The plots were produced using the C code written by Sa Xiao.

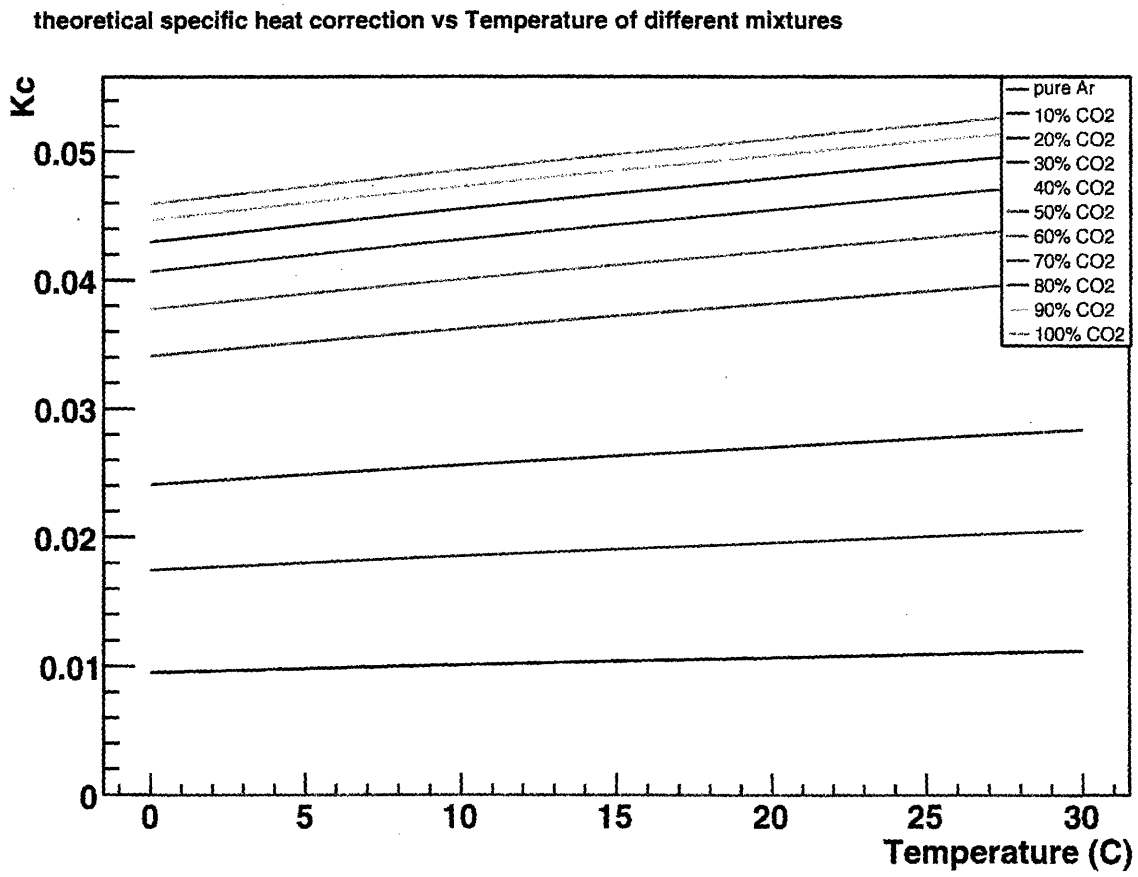

Figure A-1: Theoretical curves for specific heat correction as a function of temperature.

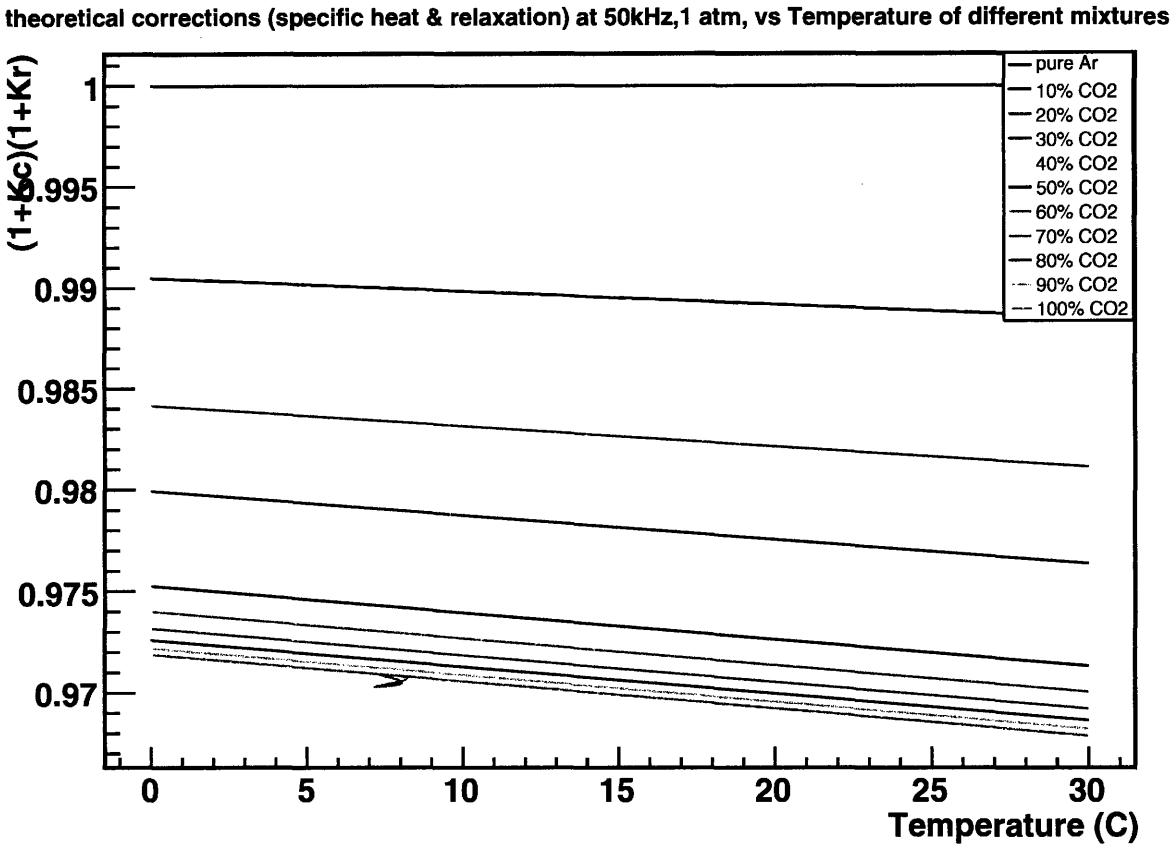

Figure A-2: Combined theoretical correction for specific heat and relaxation at 1 bar and 50 kHz for different mixtures.

Bibliography

[1] B. M. Demirkoz, *A Transition Radiation Detector and Gas Supply System for AMS*, MIT (2004).

[2] M. Mersenne, *De l'Utilite de l'Harmonie*, *Part de l'Harmonie Universelle*, Cramoisy, Paris (1636).
(Translation in J. Hawkins, *General History of the Science and Practice of Music* (3 vols.), Novello, London (1776); supplementary volume 1852, 6th ed. (1875).)

[3] A. J. Zuckerwar, *Handbook of the Speed of Sound in Real Gas*, Academic Press (2002).

[4] op. cit., Table 3.1

[5] op. cit., Chapter 4

[6] op. cit., page 95

[7] op. cit., page 103

[8] op. cit., Table 4.1, 4.2

[9] op. cit., Chapter 5

[10] op. cit., Table 5.5

[11] op. cit., Chapter 16.4.3

[12] Turk. J. Chem, 26 (2002)

[13] op. cit., Chapter 16.4.3

[14] Zuckerwar, ibid, Chapter 16.4.4

[15] op. cit., Chapter 16.4.5

[16] Specification ndd ASIC A1-A4, ndd Medizintechnik, Zurich (2003).